



## OPEN

Effect of grain orientations of Cu seed layers on the growth of  $\langle 111 \rangle$ -oriented nanotwinned Cu

Chien-Min Liu, Han-Wen Lin, Chia-Ling Lu &amp; Chih Chen

Department of Materials Science and Engineering, National Chiao-Tung University, Hsinchu, 30010 Taiwan (ROC).

We investigate the growth of Cu films on two different Cu seed layers: one with regular  $\langle 111 \rangle$ -oriented grains and the other with very strong  $\langle 111 \rangle$ -preferred orientation. It is found that densely-packed nanotwinned Cu (nt-Cu) can be grown by pulsed electroplating on the strong  $\langle 111 \rangle$ -oriented Cu seed layer without a randomly-oriented transition layer between the nt-Cu and the Cu seed layer. The electroplated nt-Cu grow almost epitaxially on the seed layer and formed  $\langle 111 \rangle$ -oriented columnar structures. However, with the regular  $\langle 111 \rangle$ -oriented Cu seed, there is a randomly-oriented transition layer between the nt-Cu and the regular  $\langle 111 \rangle$ -oriented Cu seed. The results indicate that the seed layer plays a crucial role on the regularity of  $\langle 111 \rangle$ -oriented nanotwinned Cu.

Due to the miniaturization and high performance requirements for microelectronic devices, the dimension of the Cu lines continues to shrink and the current density in the Cu line continues to rise. Therefore, electromigration in Cu remains to be a critical reliability issue in Cu lines<sup>1-5</sup>.

Nanotwinned Cu (nt-Cu) has drawn a lot of attention recently. It possesses excellent mechanical properties while it has the same conductivity with the Cu film without nanotwins<sup>6-13</sup>. In addition, the nt-Cu has higher electromigration resistance because the twin boundaries can retard the Cu electromigration rate<sup>14,15</sup>.

Furthermore, Ryu reported that  $\langle 111 \rangle$ -oriented Cu lines have longer electromigration lifetimes than  $\langle 200 \rangle$ -oriented Cu lines<sup>16</sup>. Therefore, it is expected that  $\langle 111 \rangle$ -oriented Cu with densely-packed nanotwins will possess high electromigration resistance for Cu interconnects. Anderoglu *et al.* have fabricated  $\langle 111 \rangle$ -oriented nt-Cu by magnetron sputtering<sup>17</sup>. However, microelectronic industry adopts electroplating to fabricate Cu lines for interconnects<sup>1</sup>.

Recently, we reported the fabrication of  $\langle 111 \rangle$ -oriented nt-Cu by direct current electroplating<sup>18,19</sup>. In our previous study, we use DC electroplating to deposit nt-Cu films on strong  $\langle 111 \rangle$ -oriented Cu seed layers. However there is a randomly-oriented transition layer between the nt-Cu and the Cu seed layer<sup>18,19</sup>. The randomly-oriented transition layer had no nanotwins and this layer decreased the regularity of the nt-Cu films. If the films are adopted for interconnects, the transition layer may become the weakest point for electromigration. Therefore, how to eliminate the randomly-oriented transition layer is an important issue. For the electroplating process, Cu seed layer plays a crucial role on the growth of the  $\langle 111 \rangle$ -oriented nt-Cu. However, no studies examined the effect of seed layer orientations on the growth of nt-Cu. In this letter, we investigate the deposition of nt-Cu films by pulsed electroplating on the regular  $\langle 111 \rangle$ -preferred Cu seed layers and on a strong  $\langle 111 \rangle$ -oriented seed layer. Microstructure analysis by transmission electron microscopy (TEM) on the seed layers was performed. The results reveal that with the strong  $\langle 111 \rangle$ -preferred seed layer and pulsed electrodeposition, the randomly-oriented transition layer can be minimized.

### Results and Discussion

The seed layer plays a crucial role on the growth of  $\langle 111 \rangle$ -oriented nt-Cu. In this study, we adopted two kinds of seed layers: seed layer A with a strong  $\langle 111 \rangle$  preferred orientation and seed layer B with a regular  $\langle 111 \rangle$  preferred orientation. Their grain structure and orientation were analyzed by TEM, X-ray diffraction, and electron backscattered diffraction (EBSD). Figure 1(a) shows the plan-view TEM images for the strong  $\langle 111 \rangle$ -oriented seed layer. The average grain size was 103 nm. The corresponding selected area diffraction (SAD) pattern is presented in Fig. 1(b). The diffraction rings are indexed as Cu (220), Cu<sub>2</sub>O (110), Cu<sub>2</sub>O (111) and Cu<sub>2</sub>O (220). The Cu<sub>2</sub>O came from the Cu oxide on the surface of the seed layer. Notably, the intensity of Cu (220)

SUBJECT AREAS:  
NANOSCALE MATERIALS  
ELECTRONIC PROPERTIES AND  
MATERIALS

Received  
28 April 2014

Accepted  
30 July 2014

Published  
19 August 2014

Correspondence and  
requests for materials  
should be addressed to  
C.C. (chih@mail.nctu.  
edu.tw)

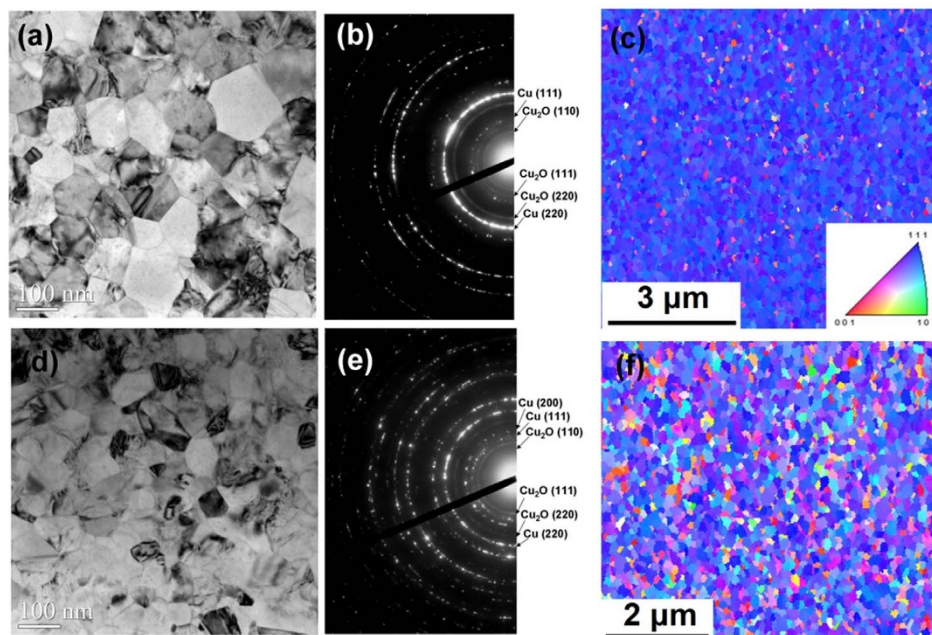


**Figure 1** | Microstructure analysis for the two Cu seed layers in this study: (a) Plan-view TEM image for the strong  $\langle 111 \rangle$ -oriented seed layer. (b) The corresponding SAD of the grains in (a). (c) Plan-view EBSD orientation image map of the strong  $\langle 111 \rangle$ -oriented seed layer. (d) Plan-view TEM image for the regular  $\langle 111 \rangle$ -oriented seed layer. (e) The corresponding SAD of the grains in (d). (f) Plan-view EBSD orientation image map of the regular  $\langle 111 \rangle$ -oriented seed layer.

was very strong and there were no detectable signals from other Cu planes. Therefore, this seed layer possesses a very strong  $\langle 111 \rangle$ -preferred orientation. Figure 1(c) presents a plan-view EBSD orientation image map for the strong  $\langle 111 \rangle$ -oriented seed layer. To calculate the percentage of  $\langle 111 \rangle$ -oriented surfaces, we defined the  $\langle 111 \rangle$ -oriented Cu surface grains that reside within  $15^\circ$  relative to

the normal of the (111) plane. The analysis indicates that 97% surface of the seed layer A resides in the (111)-preferred orientation.

On the other hand, the seed layer B has a regular (111) preferred orientation. Figure 1(d) depicts the plan-view TEM image for the seed layer B. The average grain size was measured to be 56 nm. The SAD pattern in Fig. 1(e) reveals that the Cu seed layer may be

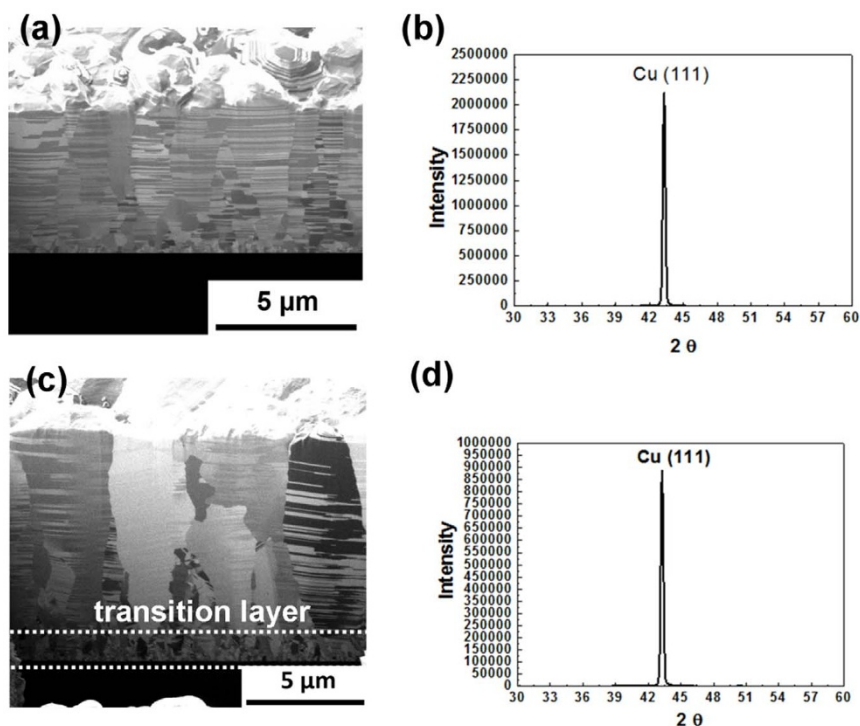


**Figure 2** | Microstructure analysis for the Cu films deposited on the two different seed layers. (a) Cross-sectional FIB image for the Cu film on the strong  $\langle 111 \rangle$ -oriented seed layer after 3000 cycles. (b) The corresponding X-ray diffraction of (a). (c) Cross-sectional FIB image for the Cu film on the regular  $\langle 111 \rangle$ -oriented seed layer after 4500 cycles. The transition layer was labeled in this figure. (d) The corresponding X-ray diffraction of (c).

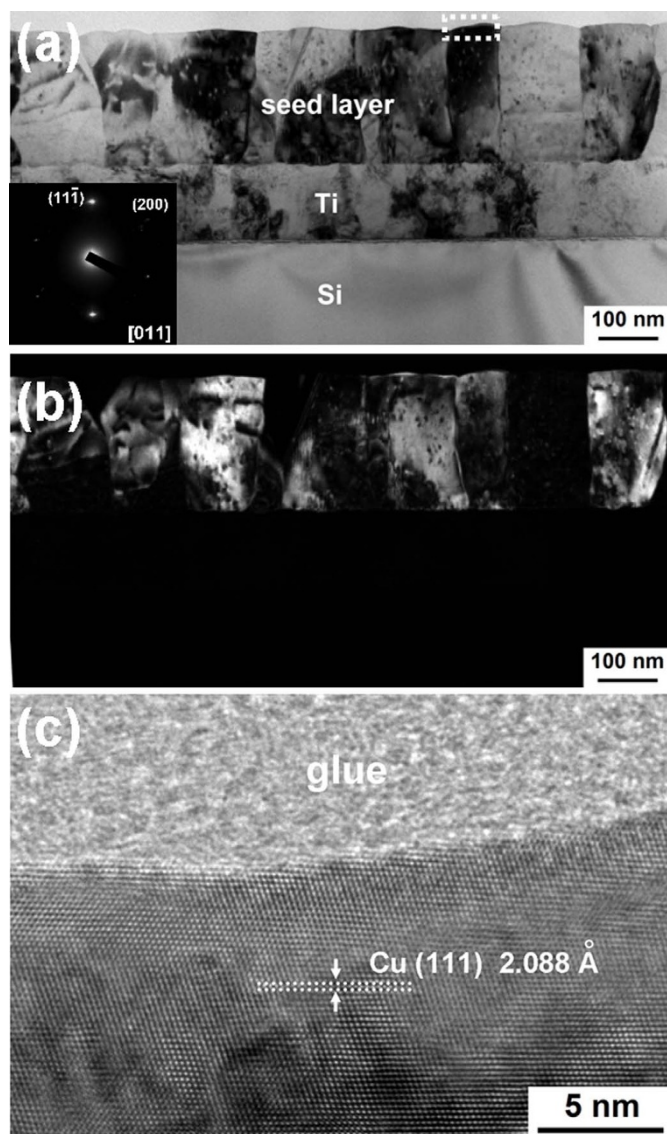


**Figure 3** | Cross-sectional TEM image for the strong  $\langle 111 \rangle$ -oriented seed layer. (a) Bright field; (b) Dark field. (c) High-resolution TEM image for the dashed rectangle area in (a).

random-oriented. Compared with the SAD pattern in Fig. 1(b), two extra diffraction rings were observed: Cu (111) and Cu (200). Figure 1(f) presents a plan-view EBSD orientation image map for the seed layer B. The results reveal that 64% of the seed layer B resides in the (111)-preferred orientation. In this paper, we denoted this seed layer as regular (111)-preferred orientation.

To produce  $\langle 111 \rangle$ -oriented nt-Cu films without a randomly-oriented transition layer, it is necessary to use a seed layer with a strong  $\langle 111 \rangle$ -preferred orientation. Figure 2(a) shows the cross-sectional FIB image for the Cu film electroplated on the strong  $\langle 111 \rangle$ -oriented seed layer A. Columnar grains with densely-packed nanotwins can be grown and there is almost no randomly-oriented transition layer between the nt-Cu film and the Cu seed layer. The nt-Cu film possesses a very strong  $\langle 111 \rangle$ -preferred orientation. The intensity of the (111) reflection is as high as 2,117,869 for the 5.8  $\mu\text{m}$  thick Cu film, as illustrated by the X-ray diffraction in Fig. 2(b). The Cu (220) reflection is invisible in the figure. The intensity ratio of (111) reflection to (220) is as high as 6051. However, when the regular-oriented Cu seed layer is used, there is a random-oriented transition layer between the nt-Cu and the Cu seed layer, as shown in the FIB image in Fig. 2(c). The thickness of this transition layer is

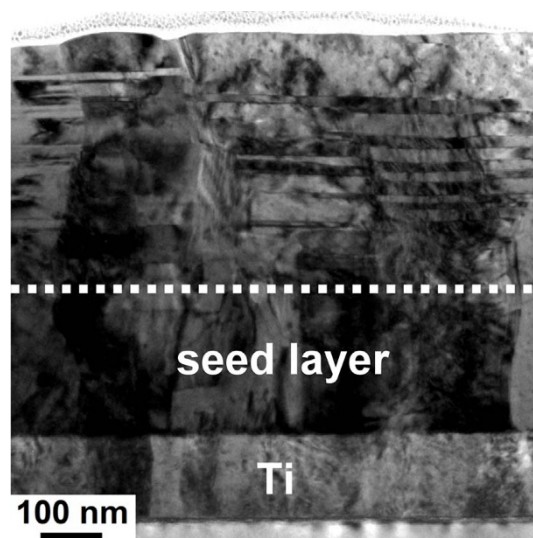


**Figure 4** | Cross-sectional TEM image for the Cu film grown on the strong  $\langle 111 \rangle$ -oriented Cu seed layer after 100 cycles.

about 1  $\mu\text{m}$ . The X-ray diffraction for this film shows that the Cu film still possesses a  $\langle 111 \rangle$ -preferred orientation as presented in Fig. 2(d). But the intensity of (111) reflection drops to 887,338 counts, which is about 42% of the nt-Cu film in Fig. 2(b). In addition, the intensity ratio of (111) reflection to (220) reflection is only 285. Thus, the Cu film in Fig. 2(c) has a weaker  $\langle 111 \rangle$ -preferred orientation than the nt-Cu film in Fig. 2(a).

Cross-sectional TEM analysis reveals that the  $\langle 111 \rangle$ -oriented seed layer possesses a columnar grain structure. Figure 3(a) shows the cross-sectional TEM images for the 200 nm seed layer A on the Ti adhesion layer of about 100 nm thick. Almost all the Cu grains exhibit columnar structure. The SAD pattern is taken from a single grain which indicated that the Cu grain has [011] pole. Figure 3(b) shows the dark field image by selecting the diffraction point of Cu (111) in the inset of Fig. 3(a). The image reveals that most of the Cu grains are  $\langle 111 \rangle$ -oriented and they are columnar structures. Figure 3(c) presents the high-resolution TEM image for a  $\langle 111 \rangle$  Cu grain labeled by the dotted rectangle in Fig. 3(a). The Cu (111) plane is almost parallel to the Si substrate. Therefore, the Cu seed layer A consists of columnar Cu (111)-oriented grains with Cu (111) free surfaces.

To further investigate how the  $\langle 111 \rangle$ -oriented seed layer induces the growth of nt-Cu by pulsed electroplating. TEM was utilized to observe the interface between the Cu seed layer A and the electroplated Cu. Figure 4 shows the cross-sectional TEM image for a 410-nm-thick Cu film electroplated on the Cu seed layer. The dashed white line represents the original free surface of the Cu seed layer. High density of nanotwins can be grown approximately after 100 nm Cu deposition. The grain size for the initial grown Cu layer is close to that of the seed layer. Therefore, most of the Cu grains grown on the seed layer were also  $\langle 111 \rangle$ -oriented. As the electrodeposition continued, some of  $\langle 111 \rangle$ -oriented nt-Cu prevailed and grew bigger in lateral direction to about 2–3  $\mu\text{m}$  when the film grew to about 5.8  $\mu\text{m}$  thick. Therefore, we suggest the growth mechanism of the columnar nt-Cu grains was: the (111) surface planes of the seed layer provide the nucleation site during initial epitaxial growth, and then the subsequent grains grow following the Cu (111) grains. As the deposition cycle increases, the (111) nt-Cu formed subsequently. With the columnar grain structure, there was less grain boundaries in the electroplated films. Thus, the interfacial energy of the film decreases<sup>20</sup>.

It is noteworthy to mention that You *et al.* and Jang *et al.* reported that  $\langle 111 \rangle$ -oriented nt-Cu films can be electroplated on Ti



substrate and Au film, respectively<sup>21,22</sup>. With a Ti seed layer, <111>-oriented nt-Cu can be fabricated by pulsed electroplating<sup>21</sup>. However, the regularity of the Cu film was not as good as the film in this paper, which employed <111>-oriented Cu seed layer. On the other hand, single-crystal nt-Cu nano pillars can be grown on the Au seed layer<sup>22</sup>. The microstructure of the Au layer is not revealed in the literature. Therefore, the nt-Cu electroplating on the Ti and Au seed layers requires more study.

## Conclusions

In summary, we have investigated the effect of grain structures of two different seed layers on the growth of nt-Cu during pulsed electroplating. By using the strong <111>-oriented Cu seed layer, densely-packed columnar nt-Cu can be grown epitaxially on the <111> grains of the Cu seed layer. However, when using the regular <111>-oriented Cu seed layer, there is a randomly-oriented transition layer between the nt-Cu and the Cu seed layer. Therefore, the seed layer play a crucial role on the formation of highly-ordered <111>-oriented nt-Cu films.

## Methods

Two sets of Cu seed layers were prepared by sputtering: one with highly <111>-preferred orientation by sputtering (seed layer A) and the other with regular <111>-oriented seed layer by sputtering (seed layer B). Before the electroplating of Cu, the Cu seed layer is dipped in citric acid for 30 s to remove the copper oxide. The process details for electrodeposition were reported in our previous publication<sup>18,19</sup>. The electroplating bath comprised a high-purity CuSO<sub>4</sub> solution composed of 0.8 M Cu cations, 40 ppm HCl and surfactants. The Cu film was electroplated by pulsed plating. In each cycle of the pulsed plating, the plating was turned on with a 50 mA/cm<sup>2</sup> current density for 1 s, i.e., T<sub>on</sub> = 1 s, and then, the current density was decreased to 0, and the electroplating was turned off for 4 s, i.e., T<sub>off</sub> = 4 s. The stirring speed of the electrolyte is 600 rpm. The microstructures of the of the Cu seed layer were examined with a JEOL-2100 scanning transmission electron microscope (STEM). The STEM examinations were performed at 200 kV with a point-to-point resolution of 0.23 nm and a lattice resolution of 0.14 nm. The microstructure and preferred orientation of the electroplated Cu films were examined by focus ion beam (FIB) and X-ray diffraction. To examine the grain orientation of the Cu seed layer, EBSD analysis was performed using a JEOL7001 field emission scanning electron microscope with an EDAX electron back-scatter diffraction system.

- Hu, C. K. *et al.* Copper interconnections and reliability. *Mat. Chem. Phys.* **52**, 5–16 (1998).
- Rosenberg, R. *et al.* Copper metallization for high performance silicon technology. *Ann. Rev. Mat.* **30**, 229–262 (2000).
- Thompson, C. V. *et al.* Electromigration and IC interconnects. *MRS Bulletin XVIII* **12**, 19 (1993).
- Hauschildt, M. *et al.* Analysis of electromigration statistics for Cu interconnects. *Appl. Phys. Lett.* **88**, 211907 1–3 (2006).
- Tu, K. N. Recent advances on electromigration in very-large-scale-integration of interconnects. *J. Appl. Phys.* **94**, 5451–5473(2003).
- Lu, L. *et al.* Ultrahigh Strength and High Electrical Conductivity in Copper. *Science* **304**, 422–426 (2004).
- Lu, L. *et al.* Revealing the Maximum Strength in Nanotwinned Copper. *Science* **323**, 607–610 (2009).

- Lu, L. *et al.* Superplastic Extensibility of Nanocrystalline Copper at Room Temperature. *Science* **287**, 1463–1466 (2000).
- Lu, K. *et al.* Strengthening Materials by Engineering Coherent Internal Boundaries at the Nanoscale. *Science* **324**, 349–352 (2009).
- Lu, L. *et al.* Nano-sized twins induce high rate sensitivity of flow stress in pure copper. *Acta Mater.* **53**, 2169–2179 (2005).
- Hodge, A. M. *et al.* Twin stability in highly nanotwinned Cu under compression, torsion and tension. *Scr. Mater.* **66**, 872–877 (2012).
- Zhang, X. *et al.* Superior thermal stability of coherent twin boundaries in nanotwinned metals. *Scr. Mater.* **66**, 860–865 (2012).
- Chen, X. H. *et al.* Grain size dependence of tensile properties in ultrafine-grained Cu with nanoscale twins. *Scr. Mater.* **64**, 311–314 (2011).
- Chen, K. C. *et al.* Observation of atomic diffusion at twin-modified grain boundaries in copper. *Science* **321**, 1066–1069 (2008).
- Liao, C. N. *et al.* In situ transmission electron microscope observations of electromigration in copper lines at room temperature. *Appl. Phys. Lett.* **87**, 141903 1–3 (2005).
- Changsup, R. *et al.* Effect of Texture on the Electromigration of CVD Copper. *Proceedings of IEEE International Reliability Physics Symposium*, 201–205 (1997).
- Anderoglu, O. *et al.* Epitaxial nanotwinned Cu films with high strength and high conductivity. *Appl. Phys. Lett.* **93**, 083108 1–3 (2008).
- Hsiao, H. Y. *et al.* Unidirectional Growth of Microbumps on (111)-Oriented and Nanotwinned Copper. *Science* **336**, 1007–1010 (2012).
- Liu, T. C. *et al.* Fabrication and Characterization of (111)-Oriented and Nanotwinned Cu by Dc Electrodeposition. *Cryst. Growth Des.* **12**, 5012–5016 (2012).
- Lu, L. *et al.* Ultrahigh strength and high electrical conductivity in copper. *Science* **304**, 2–426 (2004).
- You, Z. S. *et al.* Tensile behavior of columnar grained Cu with preferentially oriented nanoscale twins. *Acta Mater* **59**, 6927–6937 (2011).
- Jang, D. *et al.* Deformation mechanisms in nanotwinned metal nanopillars. *Nature Nanotech.* **7**, 594–601 (2012).

## Acknowledgments

Financial support from the National Science Council, Taiwan, under the contract of NSC 99-2221-E-009-040-MY3 is acknowledged.

## Author contributions

C.M.L. contributed to sample fabrication, TEM analysis, and co-wrote the paper. H.W.L. contributed EBSD experiments and analyses. C.L.L. contributed to XRD analyses. C.C. led the study and wrote the paper.

## Additional information

**Competing financial interests:** The authors declare no competing financial interests.

**How to cite this article:** Liu, C.-M., Lin, H.-W., Lu, C.-L. & Chen, C. Effect of grain orientations of Cu seed layers on the growth of <111>-oriented nanotwinned Cu. *Sci. Rep.* **4**, 6123; DOI:10.1038/srep06123 (2014).



This work is licensed under a Creative Commons Attribution-NonCommercial-NoDerivs 4.0 International License. The images or other third party material in this article are included in the article's Creative Commons license, unless indicated otherwise in the credit line; if the material is not included under the Creative Commons license, users will need to obtain permission from the license holder in order to reproduce the material. To view a copy of this license, visit <http://creativecommons.org/licenses/by-nc-nd/4.0/>